Available online at www.sciencedirect.com

ScienceDirect

Procedia CIRP 75 (2018) 279–284

www.elsevier.com/locate/procedia

15th CIRP Conference on Computer Aided Tolerancing – CIRP CAT 2018

Shape Error Modelling and Analysis by Conditional Simulations of Gaussian Random Fields for Compliant Non-Ideal Sheet Metal Parts

Manoj Babu*[a], Pasquale Franciosa[a], Darek Ceglarek[a]

[a] *WMG, University of Warwick, Coventry CV4 7AL, United Kingdom*

* Corresponding author. Tel.: +44-024-765-74501; *E-mail address:* m.k.babu@warwick.ac.uk

Abstract

Accurate modelling of geometric and dimensional errors of sheet metal parts is crucial in designing correct GD&T and preventing unnecessary design changes during the development and launch of a new assembly process. A novel conditional simulation based methodology to probabilistically model and generate non-ideal sheet metal part geometric variations is developed. The methodology generates part geometric variations, which accurately emulate part fabrication process in terms of covariance of generated deviations. The methodology uses as inputs one or more of the following: measurement data of current parts, historical measurements of similar parts or FEM-based simulations. The proposed methodology emulates real processes and products accurately by generating non-ideal part representatives based on the aforementioned input data. Results provide an easy engineering interpretation to the designer. The methodology is demonstrated using automotive door hinge reinforcement.

Peer-review under responsibility of the Scientific Committee of the 15th CIRP Conference on Computer Aided Tolerancing - CIRP CAT 2018.

Keywords: Non-ideal part modelling; Conditional simulation; Gaussian Process Regression; Variation simulation.

1. Introduction

Achieving zero defects in manufacturing necessitates simulations that can emulate real processes and products accurately. Such simulations heavily rely on accurate representation of non-ideal parts, i.e. *actual manufactured parts with geometric and dimensional errors caused due to uncertainties in manufacturing processes*. While some have dealt with non-ideal part generation [1–3], nonetheless the methodologies have neglected form tolerances which are essential for optimal tolerance specification [4], thereby yielding limited results, since neglecting form tolerances can potentially lead to non-conforming assemblies [5,6].

Sheet metal parts produced by forming, often suffer from splitting, wrinkling, shape changes due to springback and surface defects [7]. From an assembly perspective springback and surface defects are important; with springback being classified as a global defect, widely understood as deformations that affect large or the entire part; and surface defects being classified as local defect, meaning deformations that affect a small/localised region of the part.

Existing non-ideal part variation modelling methodologies considering form variation, can be classified into two main groups: (1) Morphing based, and (2) Deviation decomposition based. In morphing based methodologies, either a discrete surface representation such as mesh and Cloud of Points (CoP), or continuous parametric representation such as Bezier, NURBS, are modified to generate non-ideal parts. In contrast, deviation decomposition based methodologies decompose the measurement data into a linear combination of orthogonal modes, and are applicable to discrete surface representations only. While morphing methodologies can handle both local deformations and global deformations, deviation decomposition techniques are global deformation modelling techniques.

A constrained deformation [8] based mesh morphing methodology was proposed in [9], the methodology while being designer friendly needs the region of influence of deformation to be found, which is a non-trivial task. Skin model shapes [10], i.e. *finite skin model representatives of non-ideal parts*, based on skin model philosophy [11], is a framework to generate non-ideal parts and can be seen as belonging to both morphing and deviation decomposition methodologies. Various morphing based skin model shapes generation approaches are described in [10], and deviation decomposition based skin model shapes generation using principal component analysis is described in [12].

Existing methodologies involving skin model shapes generation do not: (1) model local deviation, and (2) define robust methodology to find correlation lengths. However, they require additional modelling effort to handle surface continuities at edges [13].

Natural mode analysis [14] decomposes deviation data into linear combination of modes based on natural modes of vibration. Geometric modal analysis (GMA) [15,16] an extension of

2212-8271
Peer-review under responsibility of the Scientific Committee of the 15th CIRP Conference on Computer Aided Tolerancing - CIRP CAT 2018.
10.1016/j.procir.2018.04.023

Statistical Modal Analysis (SMA) [17,18] utilises 3D-Discrete Cosine Transform (DCT) to decompose measurement data into linear combination of orthogonal modes. GMA has been applied to optimise fixture design [19] and link manufacturing process parameters to part form variation [20].

In addition to the inability of above mentioned deviation decomposition based methodologies to model local part deformations, the modes used in the decomposition of deviation data, usually lie in a low dimensional space, which is not easily physically interpretable. Additionally, the deviation decomposition methodologies require availability of measurement data, thus, cannot be used during early design phase. A summary of capabilities of all discussed non-ideal part form variation modelling methodologies is presented in Table 1.

Table 1: Capabilities of part form variation modelling methodologies

		Methodologies				
		Natural mode decomposition [14]	**Geometric Modal Analysis** [15,16]	**Skin Model Shapes** [11][13]	**Morphing mesh** [9]	**Proposed approach**
Part form variation modelling capabilities	Represent global deviation	✓	✓	✓	✓	✓
	Represent local deviation	×	×	×	✓	✓
	Ensure surface continuities at edges	×	×	×	✓	✓
	Probabilistic bounds on deviation	×	×	×	×	✓

As afore-discussed literature shows that the existing methodologies individually lack the ability to: 1) model simultaneously both global and local deformation, (2) ensure surface continuities at edges, and (3) provide easy engineering interpretation of the model parameters, and thus, are not designer friendly. In the present paper, a conditional simulation based non-ideal part modelling and generation methodology is proposed. The methodology overcomes aforementioned drawbacks and in addition introduces a novel probabilistic view on deviation modelling. The contributions of the study are: (1) the ability to generate both local and global part deformations, (2) a designer friendly/intuitive form variation generation methodology with physically meaningful model parameters, and (3) providing probabilistic bounds on generated part deviations.

The rest of the paper is organised as follows; Section 2 describes the problem and the proposed methodology in detail. Section 3 provides details on the application of the proposed methodology on an automotive door component. Finally, Section 4 discusses conclusion and further research.

2. Problem formulation and methodology

This study proposes a non-ideal compliant sheet metal part shape error modelling and analysis methodology by conditional simulation of Gaussian Random Fields (GRF). Each non-ideal part instance is generated through conditional simulation, which is a spatially consistent Monte Carlo simulation with the goal of realistically mimicking spatial variation of the source deviations [21].

The deviation of the manufactured part from its nominal surface is modelled as a GRF, which is characterised by its mean function and the covariance function. A detailed description of GRF can found in [22–26].

Representing the co-ordinates of nominal points on the surface of the part by a $N \times 3$ matrix $\mathbf{X}$, and the surface normal deviation of the nominal points by a $N \times 1$ vector Z. The deviation Z, is modelled as a GRF $f()$, with $\mathbf{X}$ as its input domain i.e. $Z = f(\mathbf{X})$, and non-ideal part instances are generated through conditional simulation.

Conditional simulation is performed by fixing surface normal deviations from nominal to predetermined values for predetermined key points, and then predicting deviations of all other points for the rest of the part. Detailed explanation for selection and setting of deviations of key points is presented in Section 2.2.

An illustration of a conditional simulation with two dimensional input space is presented in Fig. 1. Five possible conditional simulations of the 2D surface, considering the magnitude of deviation fixed at highlighted points, is shown superimposed in Fig. 1(a). Figure 1(b) shows the cross-section at the plane illustrated in Fig. 1(a).

The conditional simulation follows predetermined values at selected key points and the behaviour of the predicted surface between the key points is dependent on the parameters of the GRF whose optimised values are obtained for a given part as described in Section 2.1.2.

The uncertainty of the predicted deviation between key points is obtained as described in Section 2.2.3 and provides an envelope within which, statistically, all generated non-ideal part instances will lie with a given confidence. A 95% confidence interval on the mean value of generated deviations for the illustrated case is shown superimposed with the cross-sections in Fig. 1(b).

The variation of uncertainty in predicted deviations is physically meaningful, as the shapes a part can take around the fixed key point is limited due to geometric covariance [27] and the possibilities increase as we move away from the key point. Accordingly, the uncertainty of prediction is low near the key point and increases further away from it as shown in Fig. 1(b).

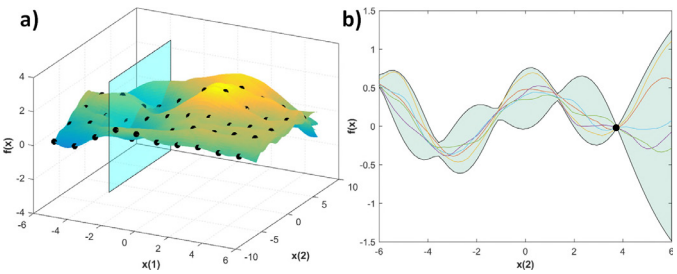

Fig. 1: Conditional simulations (a) generated surfaces; (b) surface cross-sections at shown plane with 95% confidence interval on the mean of prediction

The proposed non-ideal part modelling methodology is schematically illustrated in Figs. 2 and 3, and has two main components: (1) Non-ideal part modelling, and (2) Non-ideal part generation.

2.1. Non-ideal part modelling

During the non-ideal part modelling phase, the parameters of the GRF characterising the variation of a given part, i.e. *the mean and covariance functions*, are found. The mean func-

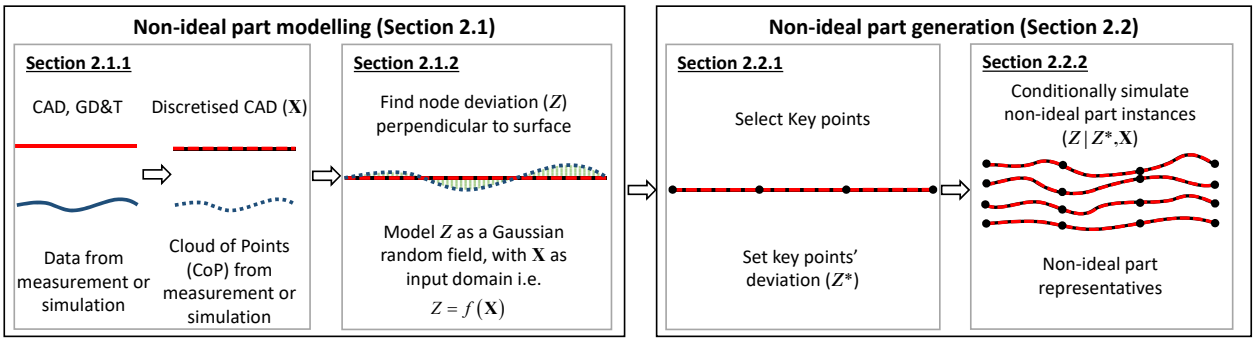

Fig. 2: Graphical illustration of methodology

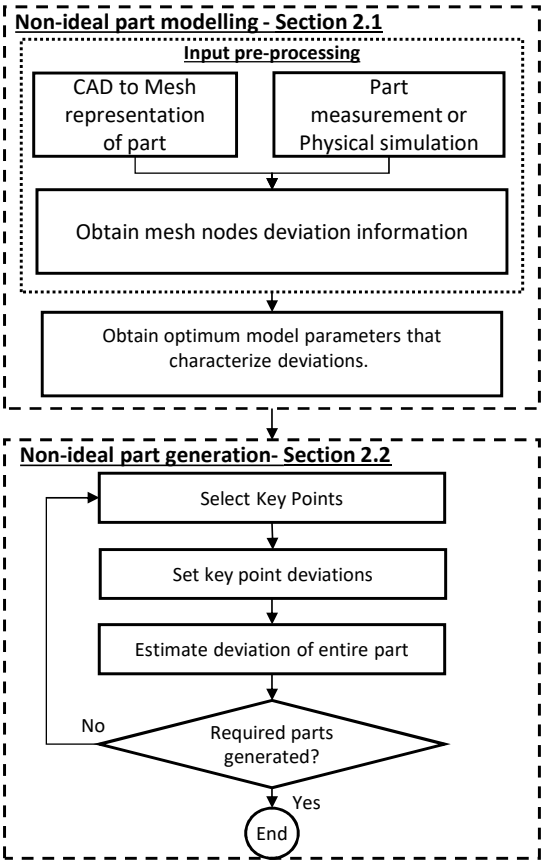

Fig. 3: Proposed non-ideal part modelling methodology

tion $m(x)$ is defined as $\mathbb{E}[f(\mathbf{x})]$. The covariance function between two points $\mathbf{x}_i, \mathbf{x}_j$, on the surface of the part, represented as, $c(\mathbf{x}_i, \mathbf{x}_j)$ is defined as $\mathbb{E}[(f(\mathbf{x}_i)-m(\mathbf{x}_i))(f(\mathbf{x}_j)-m(\mathbf{x}_j))]$, where $\mathbb{E}$ is the expectation operator.

The mean function captures large scale trends in the deviation data and can be found by fitting regression models [28], or, by the maximisation of marginal likelihood as described in Section 2.1.2. In the study a zero mean function is utilised without affecting the analysis [25], as part variations are nominally assumed to vary about zero mean.

The smoothness of generated deviations and the extent to which a given deviation propagates along a given direction (correlation length [25]), is characterised by the covariance function and its parameters. Covariance functions are classified as stationary and non-stationary [22]. Areview on the types of covariance functions with different characteristics can be found in [25].

The choice of covariance function also affects the continuity and differentiability of the generated non-ideal part representatives. While mean square continuity and differentiability of the random field is easily expressed in terms of continuity of covariance function at the origin, that of generated non-ideal part instances is a complex function of covariance function as described in [24].

In the present study we choose the covariance function to characterise the GRF instead of the variogram traditionally used in geostatistics, due to the following advantages: (1) the ability to learn and model complex patterns in data with various combinations of the covariance function [29], (2) the asymptotic properties of mean of covariance function parameters obtained in many settings through maximum likelihood estimation being equal to the true values of the parameters, and (3) the inability of the empirical semivariogram to distinguish the exact smoothness a differentiable process is [26].

For illustration purpose we choose the squared exponential covariance function represented by Eq. 1 where, for the three dimensional input case of non-ideal part modelling $\mathbf{x}$ is a 1×3 vector, σ_f^2 is the signal variance or the scaling factor [25], and, M is a 3×3 diagonal matrix with l^{-2}, the inverse of square of correlation lengths as diagonal. Representing by θ the set of all covariance function parameters $\{\sigma_f^2, l^{-2}\}$. The aim of the non-ideal part modelling phase is to find the optimum θ that fit the given part variation pattern, the optimised parameters are utilised during non-ideal part generation to emulate the part deviation correlation.

$$c(\mathbf{x}_i, \mathbf{x}_j) = \sigma_f^2 \exp\left(-\frac{1}{2}(\mathbf{x}_i - \mathbf{x}_j)M(\mathbf{x}_i - \mathbf{x}_j)^T\right) \quad (1)$$

2.1.1. Input and pre-processing

Part variation data either in the form of physical simulation of manufacturing process (for instance from FEM analysis) or measurement of manufactured part, are utilised to obtain non-ideal part deviation from nominal. The CAD model of the part, for which non-ideal part is to be generated, is discretised to a mesh representation from which, utilising the part variation data, the deviation of each node from nominal is calculated utilising routines in VRM software [30]. The nominal mesh node co-ordinates act as input $\mathbf{X}$ to the model and surface normal deviation of each node from the nominal, i.e. Z, is modelled as the function $f(\mathbf{X})$.

2.1.2. Model parameters optimisation

The covariance function parameters θ, as described in Section 2.1, control smoothness and correlation properties of the generated non-ideal part. The parameters are not as rigid as the coefficients in linear or non-linear regression models, in that a given set of covariance function parameters can give rise to a large set of non-ideal parts.

The number of parameters (θ) depend on the type of covariance function and on the number of covariance functions utilised to describe the random field. The optimum values of parameters θ are found by maximising the likelihood given the part deviation data, $L(\theta|Z^*)$. The deviation data is obtained as described in Section 2.1.1. An asterisk * is used to represent known node deviations, which during modelling stage is the set of all nodes. The method of obtaining the optimum covariance parameters by maximizing the marginal likelihood is robust and immune to over fitting [31]. In this study covariance function parameters are optimised from a single instance of non-ideal part data obtained as described in Section 3.

Finding the optimum parameters that characterise the given part variation enables accurate reproduction of source variation, as the behaviour of the generated non-ideal part between key points depends on the properties of the random field characterised by the parameters of the covariance function.

Traditionally, for mathematical ease of dealing with multiplications of numbers of very small magnitudes, log likelihoods are used instead of likelihoods, and since logarithm is a monotonically increasing function maximising log likelihood is also equivalent to maximising likelihood. For a GRF the log likelihood is given by Eq. 2 [26] where, $\mathbf{C}(\theta)$ represents the $N \times N$ data covariance matrix which is obtained by applying the covariance function (for instance Eq.1) at all the mesh points of the nominal surface, $|\mathbf{C}(\theta)|$ is the determinant of $\mathbf{C}(\theta)$, and $m(\mathbf{X}^*)$ is the mean of the random field described in Section 2.1, which is assumed to as zero in the study.

$$\begin{aligned} \ln(L(\theta|Z^*)) \quad = \quad & -\tfrac{N}{2}\ln(2\pi) - \tfrac{1}{2}\ln(|\mathbf{C}(\theta)|) \\ & -\tfrac{1}{2}(Z^* - m(\mathbf{X}^*))^T \mathbf{C}(\theta)^{-1}(Z^* - m(\mathbf{X}^*)) \end{aligned} \tag{2}$$

2.2. Non-ideal part generation

The optimum parameters of the covariance function characterising the variation of a given part, obtained as described in Section 2.1.2, are utilised to generate non-ideal part representatives using conditional simulation. Conditional simulation finds various possible instances of the variation for a given deviation setting of key points. The generated non-ideal part closely resembles the source variations from which the covariance parameters were optimised, leading to realistic non-ideal part representatives. The main steps to generate non-ideal parts are: 1) key point selection, 2) key point deviation setting, and 3) deviation prediction of the entire part. These steps are explained in detail below.

2.2.1. Key point selection

Key points are the guiding points to generate different kinds of variation, and are selected such that they uniformly cover the entire surface of the part. The key points also consist of the key characteristic points which are inspected during the assembly process. The non-ideal part generated by conditional simulation pass through the key point. Additionally, selecting surface edges as key points and setting their deviation values enable to overcome surface discontinuity issues, without any additional modelling efforts.

2.2.2. Key point deviation setting

Setting up the key points' deviation is a critical step in the methodology enabling simulation of both global and local deviations depending on the number of points manipulated. For instance, when a few points are moved as shown in Fig.5(a) and 5(b), local deformations can be simulated; and when all points are moved as shown in Fig.5(c), a global deformation can be simulated. Thus, the magnitude of deviation of the key points is dependent on design intent and the variation to be simulated.

The process of setting deviations is intuitive for the designer as a given deviation at a point on the surface of the part can be obtained by moving the corresponding key point by the same magnitude. Various kinds of design intents, such as sensitivity of variation of a particular region of a part can be easily simulated by manipulating the key points in corresponding region. The method also has the added advantage of eliminating guesswork around the degree and order of the regression, or requiring to limit to second order shapes.

2.2.3. Deviation prediction of the part

The non-ideal parts generated by conditional simulation take the deviation of key points as the fixed points through which the generated non-ideal part should pass through. The key point deviations set in Section 2.2.2, determine the type of variation i.e. *global or local*, to be simulated in non-ideal part instances.

The mean deviation of the entire part after setting the key point deviations is generated through Gaussian Process Regression (GPR) [25]. GPR is somewhat similar to the kriging approach [32], which largely ignores probabilistic interpretation of the model and of the individual parameters of the covariance function [33].

The deviation of all mesh nodes of the part given a set of key point deviation is found using Eq. 3.Here: $\mathbf{X}^*$, is the $K \times 3$ matrix of nominal key point co-ordinates where the deviation is set; $\mathbf{X}$, is the $N \times 3$ matrix of nominal co-ordinates of all mesh points of the part where deviation is to be calculated; Z^*, is the $K \times 1$ vector of key point deviations; $\mathbf{I}$, is an identity matrix with size equal to the number of key points; $\mathbf{C}(\mathbf{X}, \mathbf{X}^*)$, is the $N \times K$ covariance matrix with covariance function (Eq. 1) evaluated between each point in $\mathbf{X}$ and $\mathbf{X}^*$; $\mathbf{C}(\mathbf{X}^*, \mathbf{X}^*)$, is the $K \times K$ covariance matrix with covariance function (Eq. 1) evaluated between each point in $\mathbf{X}^*$; σ_n^2, traditionally is the nugget effect [32] or measurement error variance [25], which in the present non-ideal part modelling methodology is set to zero so that the generated non ideal part instances exactly pass through the key points. The optimum parameters of the covariance function characterising the variation of a given part found in Section 2.1.2 are utilised to evaluate the covariance matrices in Eq. 3.

$$m(f(\mathbf{X})|\mathbf{X}, \mathbf{X}^*, Z^*) = \mathbf{C}(\mathbf{X}, \mathbf{X}^*)\left(\mathbf{C}(\mathbf{X}^*, \mathbf{X}^*) + \sigma_n^2\mathbf{I}\right)^{-1} Z^* \tag{3}$$

The prediction of non-ideal part deviations using GPR additionally provides the variance of predicted deviation values (Eq. 4), thereby, enabling to determine the probabilistic bounds on generated part instances for given key point deviations. Multiple instances of non-ideal parts for given key points' setting are obtained by adding correlated random variables generated

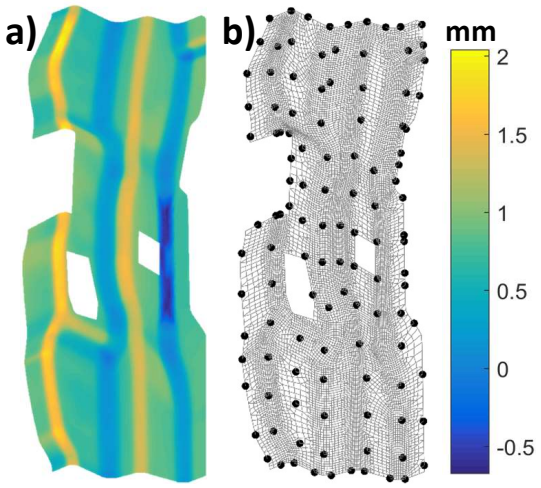

Fig. 4: a) Input pattern; b) Meshed part with key points

using the posterior covariance matrix (Eq. 4) to the mean values predicted (Eq. 3) utilising the conditional simulation methodology described in [21] which helps narrow the uncertainty by generating more probable non-ideal parts than the random variations imparted by existing methodologies [10].

Non-ideal parts with a given probability of occurrence can be generated by addition of deviations (scaled according to the chosen probability using the variance of prediction) to mean surface. Such non-ideal parts when used in assembly enable probabilistic handling of variation propagation in manufacturing processes.

$$\mathbb{V}(f(\mathbf{X})|\mathbf{X},\mathbf{X}^*,Z^*) = \mathbf{C}(\mathbf{X},\mathbf{X}) - \mathbf{C}(\mathbf{X},\mathbf{X}^*)\left(\mathbf{C}(\mathbf{X}^*,\mathbf{X}^*)+\sigma_n^2\mathbf{I}\right)^{-1}\mathbf{C}(\mathbf{X}^*,\mathbf{X}) \quad (4)$$

3. Case study

The proposed methodology is applied to automotive door hinge reinforcement. The part geometric deviation data is obtained from a single measurement of manufactured part and is illustrated in Fig. 4(a).

Firstly, the CAD model of the part for which non-ideal representatives are to be generated is discretised to its mesh representation. The meshed representation of hinge reinforcement has approximately 12000 nodes as shown in Fig. 4(b). The deviation at each node (Z^*) is found as described in Section 2.1.1. The nominal position of all mesh node points in 3-dimensions forms the input $\mathbf{X}$. In the case study a Matern covariance function with automatic relevance determination (ARD) [34] is used, and the optimum parameters θ were found by maximising the marginal likelihood (Eq. 2), through gradient descent utilising the routines provided in [35].

The generation of non-ideal parts as described in Section 2.2 is achieved through the manipulation of key points. The key points are selected to form a uniform grid structure covering the entire part, and are shown in Fig. 4b. The generated non-ideal part follows the key point, and the deviation between two key points mimics the original deviation pattern due the information carried by the covariance parameters θ.

The simulation of both local and global variations for the automotive door hinge reinforcement with the moved key points

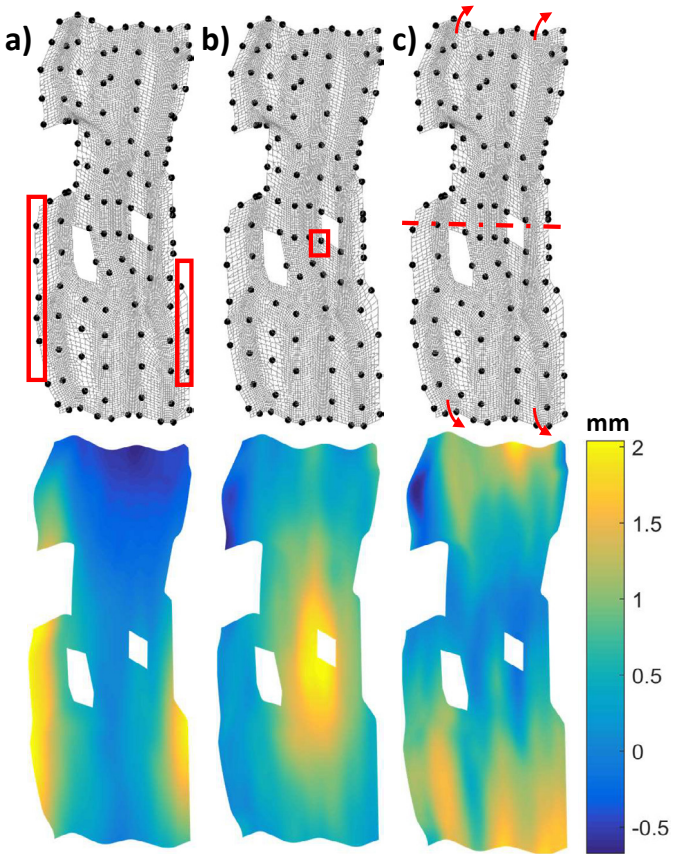

Fig. 5: a) Local defect at flanges; b) Local defect in the interior; c) Global defect - bending about illustrated axis

and corresponding non-ideal part generated is shown in Fig. 5. The key points inside the highlighted rectangles are given a deviation of 2 mm in the surface normal direction for the simulation of local defects, where: Fig.5a illustrates defect affecting the flanges, and Fig. 5(b) depicts a localised interior surface defect. Fig. 5(c) shows bending about an axis (a global defect), where all key points are imparted a deviation in the surface normal direction to simulate a bending of 0.2 rad about the illustrated axis.

The simulation of local defect is performed by moving only a few key points, in contrast for a global defect the deviation of all key points has to be specified depending on the type of defect to be simulated. Compound defects with both global and local deformations can be simultaneously simulated by superimposing the key point deviations corresponding to individual defects. Similarly setting the key-point deviations to vary according to GD&T specifications enables simulation of non-ideal parts which conform to specific tolerance requirement.

It can be clearly seen from Fig. 5 that the longitudinal correlation patterns in the input pattern (Fig. 4a) is emulated by the generated deviations. This emulation of input correlation patterns enables the generated non-ideal part representatives to be realistic representations of manufactured part.

4. Conclusions

The non-ideal part modelling and generation methodology developed in this paper can model and generate most common part variations/defects that occur in sheet metals. The method-

ology requires very few parameters to be determined by hand and the generated part form variations are similar to the source variation in terms of covariance of generated deviations, unlike random variations which existing methodologies generate. The characterisation of deviation is automatically performed by maximising the marginal likelihood, without requiring the tuning of many parameters or manual parameter guessing. The methodology is also able to model and generate non-ideal parts from a single non-ideal part data instance.

Additionally, the methodology provides: (1) probabilistic bounds on generated variation enabling us to deal with variation propagation in a probabilistic way, and (2) characterisation of covariance parameters enables generalizing the variation across different parts manufactured from a given process. However, a known issue with GPR is the increase in computational cost involved with inverting $N \times N$ matrix, where N represents the number of known data points. As future work we aim to: (1) develop a mapping from covariance function parameters to the manufacturing process parameters enabling the simulation of non-ideal part truly independent of data, either measurement or simulation; and (2) extend the methodology to characterise the non-ideal part variation in a batch of parts.

Acknowledgements

This study has been supported by the UK EPSRC project EP/K019368/1: " Self-Resilient Reconfigurable Assembly Systems with In-process Quality Improvement."

References

[1] U. Roy, C. Liu, T. Woo, Review of dimensioning and tolerancing: representation and processing, Computer-Aided Design (1991) 466–483.

[2] W. Polini, Taxonomy of models for tolerance analysis in assembling, International Journal of Production Research 50 (7) (2012) 2014–2029. doi:10.1080/00207543.2011.576275.

[3] H. Chen, S. Jin, Z. Li, X. Lai, A comprehensive study of three dimensional tolerance analysis methods, Computer-Aided Design 53 (2014) 1–13. doi:10.1016/j.cad.2014.02.014.

[4] R. S. Pierce, D. Rosen, A Method for integrating form errors into geometric tolerance analysis, Journal of Mechanical Design 130 (1) (2007) 11002. doi:10.1115/1.2803252.

[5] J. Grandjean, Y. Ledoux, S. Samper, H. Favrelière, Form errors impact in a rotating plane surface assembly, Procedia CIRP 10 (2013) 178–185. doi:10.1016/j.procir.2013.08.029.

[6] J. Grandjean, Y. Ledoux, S. Samper, On the role of form defects in assemblies subject to local deformations and mechanical loads, International Journal of Advanced Manufacturing Technology 65. doi:10.1007/s00170-012-4298-6.

[7] S. L. Semiatin, E. MArquard, H. Lampman, ASM Handbook: Metalworking - sheet forming, Vol. 14, ASM international, 2006.

[8] P. Borrel, A. Rappoport, Simple constrained deformations for geometric modeling and interactive design, ACM Transactions on Graphics 13 (2) (1994) 137–155. doi:10.1145/176579.176581.

[9] P. Franciosa, S. Gerbino, S. Patalano, Simulation of variational compliant assemblies with shape errors based on morphing mesh approach, The International Journal of Advanced Manufacturing Technology 53 (1-4) (2010) 47–61. doi:10.1007/s00170-010-2839-4.

[10] B. Schleich, N. Anwer, L. Mathieu, S. Wartzack, Skin Model Shapes: A new paradigm shift for geometric variations modelling in mechanical engineering, Computer-Aided Design 50 (2014) 1–15. doi:10.1016/j.cad.2014.01.001.

[11] ISO-17450, ISO 17450-1:2011, Geometrical product specifications (GPS) General concepts Part 1 : Model for geometrical specification (2011).

[12] M. Zhang, N. Anwer, A. Stockinger, L. Mathieu, S. Wartzack, Discrete shape modeling for skin model representation, Proceedings of the Institution of Mechanical Engineers, Part B: Journal of Engineering Manufacture 227 (5) (2013) 672–680. doi:10.1177/0954405412466987.

[13] X. Yan, A. Ballu, Toward an automatic generation of part models with form error, Procedia CIRP 43 (2016) 23–28. doi:10.1016/j.procir.2016.02.109.

[14] S. Samper, F. Formosa, Form defects tolerancing by natural modes analysis, Journal of Computing and Information Science in Engineering 7 (1) (2007) 44. doi:10.1115/1.2424247.

[15] A. Das, P. Franciosa, P. Prakash, D. Ceglarek, Transfer function of assembly process with compliant non-ideal parts, Procedia CIRP 21 (2014) 177–182. doi:10.1016/j.procir.2014.03.195.

[16] A. Das, Shape variation modelling, analysis and statistical control for assembly system with compliant parts, Ph.D. thesis, University of Warwick (2016).

[17] W. Huang, Methodologies for modelling and analysis of stream of variation in compliant and rigid assemblies, Ph.D. thesis, University of Wisconsin-Madison (2004).

[18] W. Huang, J. Liu, V. Chalivendra, D. Ceglarek, Z. Kong, Y. Zhou, Statistical modal analysis for variation characterization and application in manufacturing quality control, IIE Transactions 46 (5) (2014) 497–511. doi:10.1080/0740817X.2013.814928.

[19] A. Das, P. Franciosa, D. Ceglarek, Fixture design optimisation considering production batch of compliant non-ideal sheet metal parts, Procedia Manufacturing 1 (MAY) (2015) 157–168. doi:10.1016/j.promfg.2015.09.079.

[20] A. Das, P. Franciosa, A. Pesce, S. Gerbino, Parametric effect analysis of free-form shape error during sheet metal forming parametric effect analysis of free-form shape error during sheet metal forming, International Journal of Engineering Science and Technology (IJEST) 9 (September).

[21] J.-P. Chiles, P. Delfiner, Geostatistics: modeling spatial uncertainty, Vol. 497, John Wiley & Sons, 2009.

[22] E. Vanmarcke, Random fields: Analysis and synthesis, MIT Press Cambridge, MA., 1983.

[23] R. J. Adler, The geometry of random fields, Society for Industrial and Applied Mathematics, 2010. doi:10.1137/1.9780898718980.

[24] R. J. Adler, R. J. Adler, J. E. Taylor, K. J. Worsley, Applications of random fields and geometry: foundations and case studies, 2010.

[25] C. E. Rasmussen, C. K. Williams, Gaussian processes for machine learning, Vol. 1, MIT press Cambridge, 2006.

[26] M. L. Stein, Interpolation of spatial data: some theory for kriging, Springer Science & Business Media, 2012.

[27] K. G. Merkley, Tolerance analysis of compliant assemblies, Ph.D. thesis, Brigham Young University (1998).

[28] N. Cressie, C. K. Wikle, Statistics for spatio-temporal data, Wiley, 2011.

[29] D. Duvenaud, J. R. Lloyd, R. Grosse, J. B. Tenenbaum, Z. Ghahramani, Structure discovery in nonparametric regression through compositional kernel search, Proceedings of the 30th International Conference on Machine Learning 30 (2013) 1166–1174. arXiv:arXiv:1302.4922v4.

[30] P. Franciosa, D. Ceglarek, Fixture analyser & optimiser (2017).
URL `http://www2.warwick.ac.uk/fac/sci/wmg/research/manufacturing/downloads/`

[31] D. J. C. MacKay, Bayesian interpolation, Neural Computation 4 (3) (1992) 415–447. doi:10.1162/neco.1992.4.3.415.

[32] J.-P. Chiles, P. Delfiner, Geostatistics: modeling spatial uncertainty, 2nd Edition, Wiley-Blackwell, 2011.

[33] D. J. MacKay, Introduction to gaussian processes, NATO ASI Series F Computer and Systems Sciences 168 (1998) 133–166.

[34] R. M. Neal, Bayesian learning for neural networks, Springer New York, 1996.

[35] C. E. Rasmussen, H. Nickisch, The GPML Toolbox version 3 . 2, Toolbox (2013) 1–32.
URL `http://www.gaussianprocess.org/gpml/code/matlab/doc/manual.pdf`